



## Original article

## Surface fitting methods for modelling leaf surface from scanned data



M.N. Oqielat

Department of Mathematics, Faculty of Science, Al Balqa Applied University, Salt 19117, Jordan

## ARTICLE INFO

## Article history:

Received 9 February 2017

Accepted 27 March 2017

Available online 11 April 2017

## Keywords:

Interpolation

Finite elements methods

Virtual leaf

Radial basis function

Clough-Tocher method

## ABSTRACT

Modelling leaves accurately is important in the improvement of a virtual plant model. Therefore an accurate illustration of the leaves are important which can be achieved via mathematical models. These models can be used to study biological procedures for instance, a canopy light environment or photosynthesis. In this research we proposed a new surface fitting method called Gaussian radial basis function Clough-Tocher method (RBF-CT) for modelling a leaf surface. The Gaussian RBF-CT method strategy based on joining the Gaussian radial basis function (RBF) and Clough-Tocher (CT) methods. The accuracy of the presented method is validated by applying it to scattered data taken from Franke (1982) as well as to a real scattered data set collected using a laser scanner from an Anthurium leaf (Loch, 2004). Our method is shown to produce a realistic representation of the leaf surface.

© 2017 The Author. Production and hosting by Elsevier B.V. on behalf of King Saud University. This is an open access article under the CC BY-NC-ND license (<http://creativecommons.org/licenses/by-nc-nd/4.0/>).

## 1. Introduction

The leaves are vital in the plant development and are essential in any plant model. Our aim in this research is to construct leaf surface model based on scattered data interpolation methods to achieve a continuous surface. The interpolation methods are CT and Gaussian RBF methods.

Modelling of virtual plant has been studied by Anderson (1994), Davydov and Zeilfelder (2004), Espana et al. (1999), Prusinkiewicz (1998), Room et al. (1996), Kempthorne et al. (2015a,b), Dorr et al. (2014), Oqielat et al. (2007, 2011). Loch (2004) sampled data points using laser scanner for Elephant's ear, Anthurium, Flame and Frangipani leaves and then used finite element method to model the surface of these leaves.

In this paper we review the interpolation surface fitting methods based on the RBF and CT techniques. Then, a new hybrid RBF-CT method that combines the CT and Gaussian RBF methods is proposed. Finally, the accuracy of the RBF-CT method is assessed by applying it to a real data points collected using laser scanner from an Anthurium leaf.

The research in this paper is comprised of four main sections. In Section 2, the surface fitting techniques are given. In Section 3, the

precision of the methods are evaluated using six test functions and data points chosen from Franke (1982). The quality of the approximation of the methods is measured numerically using the maximum error and the root mean square error. In Section 4, Anthurium leaf surface is constructed using these surface fitting methods. Finally, conclusion and future work is presented in Section 5.

## 2. Surface fitting techniques

In this section, we will illustrate the RBF, CT and the Gaussian CT-RBF interpolation techniques as well as the application of the methods to two sets of data. The scattered data interpolation problem is given by:

Given  $M$  distinct scattered points  $(x_i, y_i)^T$ , and their function values  $z_i$ , find a function  $\Gamma : D \subset \mathbb{R}^2 \rightarrow \mathbb{R}$  that interpolates these data satisfying

$$\Gamma(x_i, y_i) = z_i, \quad i = 1, \dots, M. \quad (1)$$

Finite element methods consist of a triangulation (adopted in this paper) or rectangulation, where the domain is divided into subdomains and then piecewise interpolant is constructed on each element (triangle or rectangle). The value of the function is given at the vertices of the triangle and interpolation polynomial is constructed over each triangle. If the derivatives are not given then they need to be estimated. Finally, by joining the interpolant on each triangle the whole surface is then constructed. For more information see (Lancaster and Salkauskas, 1986).

E-mail address: [moaathoqily@bau.edu.jo](mailto:moaathoqily@bau.edu.jo)

Peer review under responsibility of King Saud University.



Production and hosting by Elsevier

<http://dx.doi.org/10.1016/j.jksus.2017.03.008>

1018-3647/© 2017 The Author. Production and hosting by Elsevier B.V. on behalf of King Saud University.

This is an open access article under the CC BY-NC-ND license (<http://creativecommons.org/licenses/by-nc-nd/4.0/>).

2.1. The Clough-Tocher method

The Clough-Tocher (CT) method (Clough and Tocher, 1965) is a seamed element method, where each triangle is divide into three micro-elements (subtriangles). A polynomial of degree three is then built on each micro-element to allow a continuous differentiable piecewise cubic polynomial over the whole domain, see (Oqielat et al., 2009, 2007). The form of the CT interpolant is given by:

$$\phi(x,y) = \sum_{i=1}^3 (f_i b_i + (c_i, d_i)^T \cdot \nabla f_i) + \sum_{j=1}^3 \frac{\partial f}{\partial n_j} e_j. \tag{2}$$

In this representation the twelve functions  $b_i(x,y), c_i(x,y), d_i(x,y)$  and  $e_j(x,y)$ ,  $i = 1, 2, 3$  are cardinal basis functions (Lancaster and Salkauskas, 1986). To determine  $\phi$ , twelve independent pieces of information are required which consists of the gradient and function values at each vertex as well as the edges normal directional derivative (see Fig. 1). The authors (Turner et al., 2008; Belward et al., 2008) presented analysis for the least square gradient estimation method as well as an error bounds for the method.

2.2. Radial basis functions

The approximation radial basis function  $\Gamma$  to the function  $f(x)$ , is given by:

$$\Gamma(x) = \sum_{i=1}^N a_i \mathfrak{R}(\|x - x_i\|), \quad x \in \mathbb{R}^2 \tag{3}$$

where  $r_i = \|x - x_i\|$  and  $\|\cdot\|$  is the Euclidean norm. The centres of the approximation RBF are  $x_i, i = 1, 2, \dots, N$ . If the coefficients of the RBF  $a_i, i = 1, \dots, N$  satisfies the system

$$Aa = F \quad \text{with} \quad A_{ij} = \mathfrak{R}(\|x_j - x_i\|) \quad i, j = 1, \dots, N \tag{4}$$

and  $F = (f_1, \dots, f_N)^T$ . Then  $\Gamma(x)$  is called interpolation function of  $f$  at  $x_1, \dots, x_N$ .

Radial basis function approach proposes a smooth surface to approximate the values of the function at points. This method has many application in fields for instant, hydrology (Borga and Vizzaccaro, 1997), medical imaging (Carr et al., 1997), geodesy (Junkins et al., 1971), software to drive laser scanners (Carr et al., 2001, 2003), and the partial differential equations solution (Hardy, 1990). Powell (1990) review the theory of RBF.

The computational costs in assessing the RBF to large sets of data points can become time consuming because a large compact matrix system of size  $N \times N$  has to be solved in order to calculate

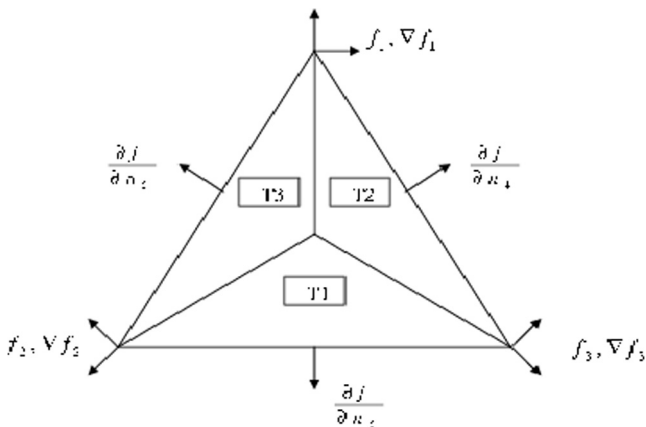


Fig. 1. The Triangle of the Clough-Tocher.

the RBF coefficients  $a_i, i = 1, 2, \dots, N$  in Eq. (4). Franke (1982), compared around 30 interpolation schemes and located that the RBFs are the most accurate methods for surface fitting. Beatson et al. (1999, 2001), Cherrie (2000) used fast evaluation techniques to reduce the computational cost of the RBF. An examples of the RBF comprise thin plate splines, Hardy’s multiquadric (Hardy, 1990) and Gaussian RBF which is adopted in this paper. The Gaussian RBF is given by:

$$\mathfrak{R}(\|x - x_i\|) = e^{-c^2 \|x - x_i\|^2}. \tag{5}$$

The accuracy of RBF interpolant depends strongly on the parameter  $c$  where this parameter is specified by the user, see for example (Carlson and Foley, 1991; Niceno, 2003; Sinoquet et al., 1998). For some values of  $c$  the problem may become ill-conditioned. Franke (1982) and Foley (1987) used  $c = 1.25 \frac{D}{\sqrt{n}}$  where  $D$  is the diameter of the minimal circle enclosing all data points.

Carlson and Foley (1991) and Franke (1982) studied the accuracy of the multiquadric and inverse multiquadric interpolant and found that the choice of the parameter  $c$  has great impact on the accuracy of the RBF. Carlson recurrent the computation of the RMS error with different choices of  $c$  and stated the optimal value of  $c$  that minimizes the RMS. Rippa (1999) performed experiments on the influence that the parameter  $c$  has on the approximation quality achieved using different RBF. Rippa proved that the value of  $c$  has impact on the quality of the RBF. Nine test functions and two sets of data are considered by Rippa. He constructed the data vector  $F = (f_1, f_2, \dots, f_N)^T$  by computing each test function over the set of data points so that

$$S(x_i) = f_i, \quad i = 1, 2, \dots, N. \tag{6}$$

An algorithm is proposed by Rippa for the choice of a good value for the parameter  $c$  that minimizes the RMS error between the RBF interpolant and the unknown function from which the data vector  $F$  was sampled. The value of  $c$  is selected by minimizing the cost function. The *mnbrak* and *brent* routines from Numerical Recipes [36] were used to do the minimization. The *mnbrak* routine is given some tolerance and two initial values  $c_1$  and  $c_2$ . It returns three numbers  $b_1, b_2$  and  $b_3$  that bracket the minimum. After bracketing the minimum, the three numbers and the tolerance parameter are passed into the function *brent* that uses Brent’s method to minimize the cost function. We refer to the minimum value of the cost function as the “good value” of  $c$ . The cost function is given by:

Let  $E$  be the vector

$$H = (H_1, \dots, H_N)^T \tag{7}$$

with

$$H_s = f_s - \Gamma^s(x_s), \quad s = 1, \dots, N, \tag{8}$$

where  $\Gamma^s$  is the interpolant to the data set with the point  $(x_s, f_s)$  removed, so that:

$$\Gamma^s(x) = \sum_{i=1, i \neq s}^N a_i^s \mathfrak{R}(\|x - x_i\|). \tag{9}$$

Rippa showed that

$$H_s = \frac{a_s}{a_s^s}, \tag{10}$$

where  $a_s$  is as defined in Eq. (6) and  $a^s$  is the solution of

$$\Lambda a^s = e^s, \tag{11}$$

where  $e^s$  is the  $s^{th}$  column of the  $N \times N$  identity matrix. Ultimately, the cost function  $C(c)$  is defined by:

$$C(c) = \|H(c)\|_1, \tag{12}$$

and

$$c_{opt} = \underset{c \in \mathbb{R}}{\operatorname{argmin}} \|H(c)\|_1. \tag{13}$$

In this research we used another way to minimize the cost function based on using the Matlab command call *fminbnd*. The *Fminbnd* return the local minimum of a single-variable function on a fixed interval using either the bisection method twice on the interval or the trisection method which divide the interval into three equal parts. One can see from our numerical result that the value of *c* obtained using *fminbnd* are comparable to the values of *c* obtained using the Rippa method.

2.2.1. The solution of the linear system  $\Lambda a = F$

The matrix  $\Lambda$  in (6) is invertible if and only if Eq. (4) has a unique solution. Micchelli (1984) propose conditions on invertibility of  $\Lambda$  that can be checked for the multiquadric RBF and Gaussian RBF. However, the approximation solution of the linear system is computed by applying the truncated singular value decomposition (TSVD) of  $\Lambda$  (Tony et al., 1990).

$$\Lambda = U \Sigma V^T = \sum_{i=1}^N u_i \sigma_i v_i^T, \tag{14}$$

where the left and right singular vectors  $u_i$  and  $v_i$  are the columns of the matrices  $U$  and  $V$ , respectively, and  $\sigma_i$  are the singular values of  $\Lambda$ .

We applied TSVD (Moroney, 2006) to castoff the small singular values regarding to the benchmark where the singular values that are equal to, or less than, the product of the largest singular value with a chosen target  $\varepsilon$  (machine epsilon) are ignored. Thus, if  $\sigma_i \leq \sigma_1 \varepsilon$  we ignore  $\sigma_i, i = 2, \dots, N$ . A new matrix  $\Lambda_t$  is then formed with rank  $t$  defined by:

$$\Lambda_t = \sum_{i=1}^t u_i \sigma_i v_i^T, \quad t \leq \operatorname{rank}(\Lambda) \tag{15}$$

and the solution to (6) is then approximated by:

$$a = \Lambda_t^\dagger F = \sum_{i=1}^t \frac{u_i^T F}{\sigma_i} v_i, \tag{16}$$

where the matrix  $\Lambda_t^\dagger$  is the pseudoinverse of the matrix  $\Lambda_t$ .

2.3. Gaussian radial basis function-Clough-Tocher method

A new radial basis function Clough-Tocher (RBF-CT) method for surface fitting is proposed in this paper. This method is based on using local Gaussian RBF or global Gaussian RBF to evaluate the gradient at the midpoints and the vertices of the Clough-Tocher triangle. The Gaussian RBF is given by:

$$\Gamma(x) = \sum_{i=1}^N a_i \mathfrak{R}(r_i),$$

where  $\mathfrak{R}(r)$  is given in Eq. (5). Then, the gradient of  $\Gamma$  is given by:

$$\nabla \Gamma(x) = \sum_{i=1}^N a_i \nabla \mathfrak{R}(r_i), \tag{17}$$

where

$$\nabla \mathfrak{R}(r_i) = \frac{x - x_i}{r_i} \mathfrak{R}'(r_i), \tag{18}$$

and  $\mathfrak{R}'$  is the Gaussian radial basis function derivative given by

$$\mathfrak{R}'(r_i) = \left( \frac{\partial \mathfrak{R}}{\partial x_k}, \frac{\partial \mathfrak{R}}{\partial y_k} \right) = \left( -2(x_k - x_i)c^2 e^{-r^2 c^2}, -2(y_k - y_i)c^2 e^{-r^2 c^2} \right).$$

2.3.1. Global and local Gaussian RBF-CT approximations

Our surface fitting method based on choosing a subset of  $n$  points (the triangles vertices) from the whole data set to produce a surface triangulation. Then the global Gaussian RBF-CT and local Gaussian RBF-CT variants are considered. In the global Gaussian RBF-CT method we constructed a global Gaussian RBF interpolant  $\Gamma_n(x)$  using these  $n$  points, subsequently  $\nabla \Gamma_n(x)$  is used to compute the gradients for all CT triangles in the mesh. On the other hand, for the local Gaussian RBF-CT method we used a local subset of size  $m$  of the  $N$  points ( $m = 20$  or  $m = 40$  in our numerical experiments) to build a local Gaussian RBF interpolant  $\Gamma_m(x)$  for each triangle.  $\nabla \Gamma_m(x)$  is then used to compute the CT triangle gradients. Note that we choose these  $m$  points to be the closest points to each of the edge midpoints and to the vertices of the CT element of interest.

The process that uses this RBF-CT method for the purpose of surface reconstruction is given in the following algorithm:

**Algorithm 1: The Gaussian RBF-CT Method for Surface reconstruction**

INPUT:  $N$  data points  $\{(x_i, f_i), i = 1, \dots, N\}$

**Step 1:** select a subset of  $n \subset N$  data points for the surface triangulation.

**Step 2:** compute the RBF linear system (4) Using either a local Gaussian RBF built on each triangle from  $m$  points OR a global Gaussian RBF from  $n$  points.

**Step 3:** use the TSVD approach to estimate the solution of the linear system

**Step 4:** construct the local or the global gradient using the coefficients of the RBF

**Step 5:** construct the surface by applying the hybrid method either locally  $\nabla \Gamma_m(x)$  Or globally  $\nabla \Gamma_n(x)$  to obtain the derivatives of the CT interpolant.

Two methods to select the parameter  $c$  for use in the Gaussian RBF were investigated. The first method based on using the algorithm of Rippa either globally or locally while the second method based on using the Matlab command *Fminbnd* given in Section 2.2. In the global strategy, a total of  $n = 100$  points (all points) are used to create one global value of  $c_{opt}$  for all CT elements; whereas in the local approach, a total of  $m = 20$  or  $m = 40$  points are used to obtain a local estimate of  $c_{opt}$  for each CT element.

3. Numerical Investigation for the Franke data set

The mathematical technique given in Section 2 is assessed using numerical experiments presented in this section. To evaluate the accuracy of these methods we used six test functions and two subsets of data taken from Franke (1982). The first subset contains 33 points used to assess the accuracy of the methods by computing the root mean square error (RMS) given in Eq. (19), while the second subset consist of 100 data points which are used to construct the triangulation of the surface, see Oqielat et al., 2009, 2007).

$$\operatorname{RMS} = \sqrt{\frac{\sum_{i=1}^q [Z(a_i, b_i) - f(a_i, b_i)]^2}{q}}, \tag{19}$$

where  $f(a_i, b_i)$  is the exact value of the function and  $Z(a_i, b_i)$  is the estimate value at the equivalent points.

3.1. Gaussian radial basis function Clough-Tocher method

As mentioned before, the gradients of the CT element are not given, we applied the global Gaussian RBF approach that uses all  $N = 100$  data points and the local Gaussian RBF approach that use  $m = 20$  or  $m = 40$  data points to compute the gradient of the

CT triangle for the Franke data. The parameter  $c$  in the two cases was approximated either globally using the  $n = 100$  data points (Table 3), or locally using a selection of  $m = 20$  or  $m = 40$  neighbouring points for each CT triangle (Table 4). Tables 2 and 3 show the RMS errors for the six test functions using the global and local RBF-CT method where the parameter  $c$  computed using Rippla method. We observe that the RMS errors in both cases are almost as good as the exact values given in Table 1. Moreover, the RMS errors obtained using the global RBF-CT method appear similar to those produced using the local RBF-CT method. The parameter  $c$  computed using global method is less computationally costly than using  $c$  locally because a new value of  $c$  must be calculated each time the local RBF is constructed. Table 3 shows as expected the global values of  $c$  were always contained in the local ranges of  $c$  given for each of the functions.

Another observation from Tables 2 and 3 was that the RMS error produced using the local RBF-CT method constructed with  $m = 40$  points was always found to be more accurate than the RMS produced for the surface representation constructed from  $m = 20$  points (for both cases whether  $c$  is approximated globally or locally). Furthermore, it appears from our numerical experimentation for the Franke data that the local gradient estimates obtained when  $m = 40$  using a globally determined value of  $c$  would be the most computationally competitive of all of our methods when  $m$  is large.

In fact the Gaussian RBF-CT method gives RMS errors quite close to the case where the exact gradient is used (see Table 1). We now carry this finding to the next section and explore the suitability of the Gaussian RBF-CT surface fitting strategy for a real leaf data set.

By profiling the codes in Matlab, we observed for the local and global RBF-CT methods that most of the computational time was spent in solving the gradient RBF problems via the TSVD. In conclusion, we found that the global Gaussian RBF-CT method was the most efficient of all methods tested, followed by the local Gaussian RBF-CT method.

#### 4. Application of the Gaussian RBF-CT method to a leaf data set

A set of points collected from real surface of a leaf are required to be able to reconstruct the leaf surface. To evaluate the accuracy of the Gaussian RBF-CT technique, the Gaussian RBF are used to estimate the gradients of the clough-Tocher triangle for the Anthurium leaf triangular mesh (Loch, 2004). The data of the Anthurium leaf comprises of 4,688 leaf surface points and 79 boundary points, see Fig. 2.

Now to apply the Gaussian RBF-CT method to the Anthurium data, a new reference plane for the data as well as a triangulation for the surface of the leaf are required, see (Oqielat et al., 2009, 2007).

##### 4.1. Reference plane of the leaf data

The leaf data points reference plane may not essential correspond with the  $xy$ -plane in the coordinate system of the data points. To solve this issue a least squares fit to the leaf points is then used as reference plane and then rotating the coordinate system to obtained the  $xy$ -plane as the new reference plane. To achieve the rotations we need at first rotating the reference plane normal vector about the  $y$ -axis into the  $yz$ -plane and then rotating

about the  $x$ -axis into the  $xz$ -plane, for more details about this procedure, see Oqielat et al. (2007, 2009).

##### 4.2. Leaf surface triangulation

A subset of the Anthurium leaf data set ( $N = 4688$  points) is selected to reduce the computational cost for surface fitting, these subset are used to generate a triangulation of the surface of the leaf using software written in the C language by Niceno (2003) called *EasyMesh* mesh generator. *EasyMesh* produce two-dimensional *Delaunay* and constrained *Delaunay* triangulations in general domains. If the domain is convex then a better quality triangulation can be achieved. *EasyMesh* was not capable to create the wanted triangulation because the 79 Anthurium leaf boundary points do not represent a convex set. To solve this issue we employed an algorithm (Sedgewick, 1988) to produce the convex hull, this algorithm return 49 points. After that, the closest points to these 49 points from the original 79 boundary points were then found using *dsearch* which is *Matlab* command. As a result of this process the convex domain shown in Fig. 4(a) is defined using 38 boundary points.

To facilitate *EasyMesh* to construct fewer and better formed triangles we can define either a vertical line or horizontal or in the inner of the convex hull. Its appear that the vertical line produced a more appropriate triangulation for the Anthurium leaf.

The following steps are applied to generate the triangulation of the Anthurium leaf using *EasyMesh*:

**Step 1:** An input file that consists of the vertical line description, the 38 boundary points and the length of the triangle edge for the mesh elements is provided to the *EasyMesh*. A node file that contained an extra 28 boundary points (introduced during the meshing process) to the original boundary points is return from *Easymesh* in addition to 146 internal points (vertices of the mesh) distributed inside the leaf shown in Fig. 4(a).

**Step 2:** We imported the node file that we got in step 2 into *Matlab* and then the closest points in the leaf data set were located from the internal points generated in step 1 using *dsearch*. These resulting points were used as the triangle vertices of the leaf surface mesh structure.

**Step 3:** The surface values of the nearest points from the leaf data points to the *EasyMesh* boundary points are used as the boundary points of the leaf for which we do not have surface values.

**Step 4:** The leaf data points that were got from steps 2 and 3 are then used to construct the surface triangulation using the *Matlab* command *delaunay*. These four steps produce the final triangulation for the leaf surface shown in Fig. 4(b).

After we generated the triangulation of the Anthurium leaf surface, we applied the local and global Gaussian RBF-CT methods to generate the leaf surface where the gradients at the triangles edge midpoints and the vertices are approximated using the Gaussian RBF (shown in Fig. 3). The *global RBF-CT approach* based on using the triangulation points to built one global Gaussian RBF and then using it to compute the gradients at the midpoints and vertices of whole triangles in the leaf surface. The *local Gaussian RBF-CT approach* is based on selecting the closest 30 points to the triangle center and to each of the triangle vertices and then built one local Gaussian RBF from the 120 points on each triangle. This local Gaussian RBF is then used to estimate the gradient at the midpoints and

**Table 1**  
The precise gradients for the Franke functions.

Function	$F_1$	$F_2$	$F_3$	$F_4$	$F_5$	$F_6$
Exact Gradient	2.6e-3	2.1e-3	1.4e-4	4.1e-5	2.6e-4	8.7e-5



**Table 2**

The RMS error comparison using the global Gaussian RBF-CT ( $n = 100$  points) and local Gaussian RBF-CT interpolants ( $m = 20$  or  $m = 40$  points) for the six test functions. The parameter  $c$  was computed globally by Rippa method using the  $n = 100$  points.

Function	c	Global RBF-CT	Local RBF-CT	
			m = 40	m = 20
$F_1$	5.1410	4.1e-3	4.2e-3	6.8e-3
$F_2$	5.3375	4.9e-3	4.6e-3	3.5e-3
$F_3$	3.3918	2.1e-4	2.4e-4	5.7e-4
$F_4$	2.3529	2.1e-4	2.4e-4	2.9e-5
$F_5$	4.3286	2.1e-4	2.5e-4	5.3e-4
$F_6$	1.0750	2.0e-5	5.0e-5	4.6e-5

**Table 3**

The RMS error comparison using the local Gaussian RBF-CT interpolant ( $m = 20$  or  $m = 40$  points) for the six test functions. The parameter  $c$  was computed locally by Rippa method using the same ( $m = 20$  or  $m = 40$ ) points.

Function	Local RBF-CT (m = 40)		Local RBF-CT (m = 20)	
	$[c_{min} c_{max}]$	RMS	$[c_{min} c_{max}]$	RMS
$F_1$	[2.4813 5.1762]	2.7e-3	[0.5239 6.0677]	4.2e-3
$F_2$	[2.1843 13.0018]	4.4e-3	[0.3399 26.2243]	3.1e-3
$F_3$	[1.382 3.2387]	1.9e-4	[0.3942 3.3897]	4.2e-4
$F_4$	[2.1202 2.3270]	1.9e-4	[1.8912 2.3070]	3.9e-5
$F_5$	[3.6589 4.5927]	2.6e-4	[2.1005 10]	3.3e-4
$F_6$	[0.5724 2.7912]	2.4e-5	[0.2375 0.4812]	2.9e-5

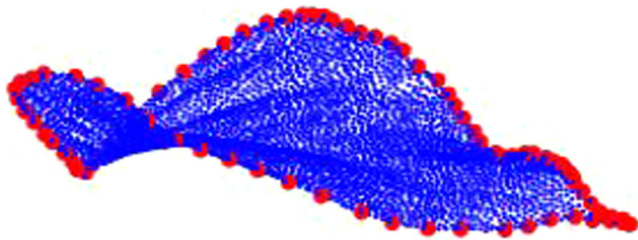


**Fig. 2.** The data points for the Anthurium Leaf. There are 79 boundary points (characterized by the larger dots) and 4,688 surface points (characterized by the smaller dots).



**Fig. 3.** The Anthurium leaf model constructed from the points (shown in Fig. 2) using the Gaussian RBF-CT technique.

vertices of the CT triangle. In both cases we used Rippa method (Rippa, 1999) to estimate the parameter  $c$  globally using the triangular mesh points. The Numerical results for these methods are given in Table 4.

4.3. Leaf surface numerical experiments

The outcome of applying the Gaussian RBF-CT technique to the data of the Anthurium leaf is given in this section. As mentioned before a subset of the leaf surface data are used for triangulation

**Table 4**

Maximum error and Relative RMS error calculated using the global and local Gaussian RBF-CT technique for the data points of the Anthurium leaf.

	Local RBF-CT	Global RBF-CT
RMS Error	0.03234	0.0194
Max. Error	0.9260	0.1206
Triangles Number	178	178
RMS Error	0.1177	0.0098
Max. Error	0.0810	0.0472
Triangles Number	391	391
RMS Error	0.0086	0.0079
Max. Error	0.5331	0.4560
Triangles Number	1486	1486

purposes, the remaining data points of the leaf data (say  $m$ ) were used to assess the method quality by two error metrics. These two error metrics are the RMS error (see Eq. (19)) and the maximum error associated with the surface fit in relation to the maximum variation in  $z$  as

$$MaximumError = \frac{\max(|S(a_i, b_i) - z_i|)}{\max(z_i) - \min(z_i)},$$

where  $z_i$  and  $S(a_i, b_i)$ ,  $i = 1, 2, \dots, m$  are respectively the given values of the function and the CT estimated values at the data points ( $m$ ).

To achieve a high accurate representation of the leaf surface and to confirm that our results were consistent as the mesh was refined, we used EasyMesh to construct three different triangulation (178, 391 and 1,486 triangles) given in Figs. 4(b) and 5(a)-(b).

Table 4 shows the maximum errors and the relative RMS using the local and global Gaussian RBF-CT techniques for the Anthurium leaf for three different triangulations, see Figs. 4 and 5. The relative RMS was calculated using:

$$RelativeRMS = \frac{RMS}{\max(z_i) - \min(z_i)}, i = 1, 2, \dots, m.$$

Note that three sets of the Anthurium leaf points were employ to measure the accuracy of the leaf surface. The first set consist of 4,427 data points where the EasyMesh triangulations contained 103 vertices (178 triangles) including 52 boundary points; While

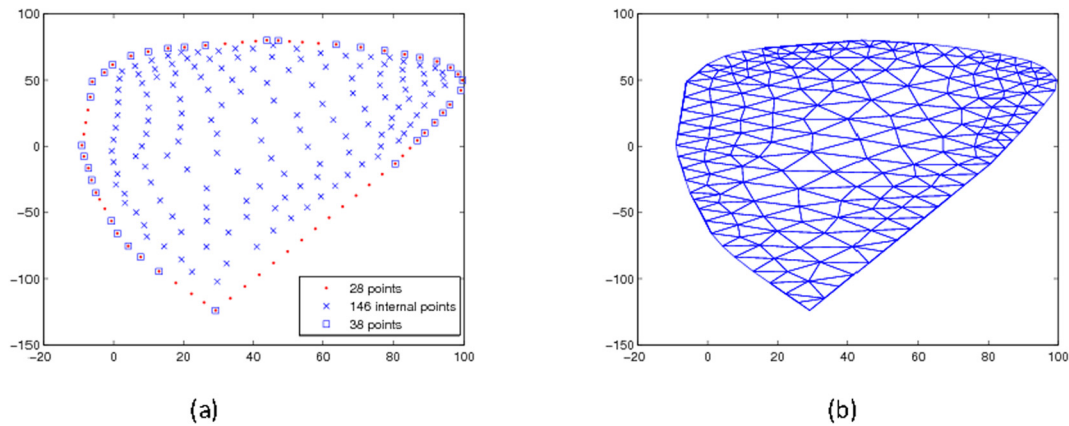


**Fig. 4.** a) The interior (Triangle vertices) and boundary points of the mesh build by Easymesh. The  $\times$  points are the 146 internal points; the dot points are the 28 extra points added by Easymesh, while The square points are the 38 boundary points that are given to Easymesh. b) Triangulation of the 212 points of the Anthurium leaf surface constructed by *EasyMesh*.

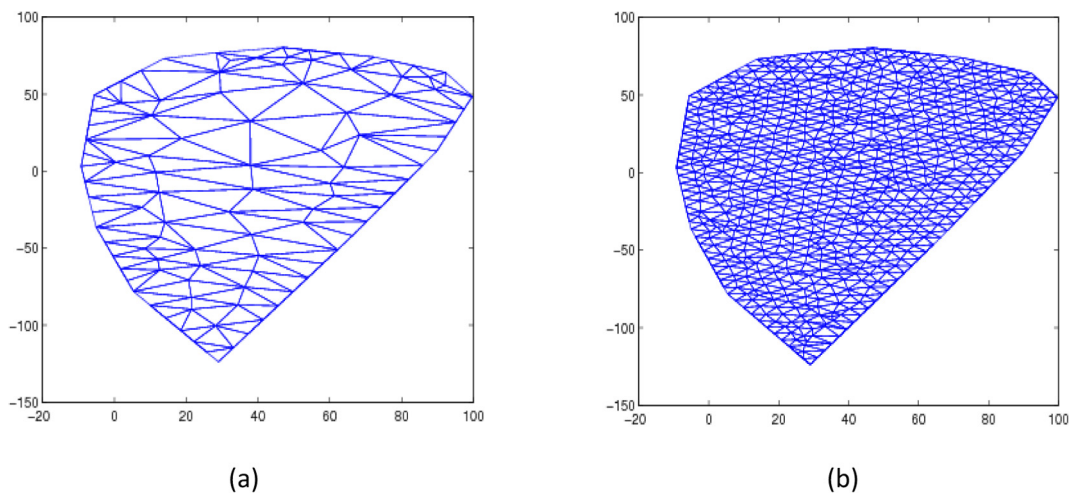


**Fig. 5.** The triangulation of the Anthurium leaf surface constructed using *EasyMesh* of (a) Rougher mesh of 103 points and (b) a improved mesh of 762 points.

the second set consist of 4,460 data points where the *EasyMesh* triangulations contained 212 vertices (391 triangles) including 66 boundary points; whereas the third set consist of 3,793 data points and the *EasyMesh* triangulations contained 762 vertices (1486 triangles) including 106 boundary points.

We observed from Table 4 that using the global Gaussian RBF-CT method gave more accurate maximum errors and RMS values than using the local Gaussian RBF-CT method in all three cases. Moreover, a more accurate representation of the surface is obtained for the global method when the number of triangular elements increases. This observation is expected and provides a reasonable justification for the Gaussian RBF-CT method for achieving the leaf surface representation.

The number of points used to build the local Gaussian RBF is important for the gradients estimate accuracy. In our research we have used the closest 30 points to the centroid of the triangle and to each vertex where the computational cost is reasonable and we got the best result, whereas using more points increase the computational expense and does not improve the accuracy much. Moreover using less points result in decreasing the precision of the fit because of inadequate points being employed to deliver a accurate local surface representation to guarantee esensible estimation of the gradient.

## 5. Conclusions

In this research, we presented a surface fitting method based on mathematics for modelling the surface of the leaf from three-dimensional scanned data points and shown that our method produce an accurate leaf surface representation. The surface representation can be used to find the path of pesticide or water droplet on a leaf surface and then to determine the effectiveness of treatment of different pesticide formulations.

## References

- Anderson, W.K., 1994. A grid generation and flow solution method for the Euler equations on unstructured grids. *J. Comput. Phys.* 110, 23–38.
- Beatson, R.K., Cherrie, J.B., Mouat, C.T., 1999. Fast fitting of c basis functions: methods based on preconditioned GMRES iteration. *Adv. Comput. Math.* 11, 253–270.
- Beatson, R.K., Cherrie, J.B., Ragozin, D.L., 2001. Fast evaluation of radial basis functions: methods for four-dimensional polyharmonic splines. *SIAM J. Math. Anal.* 32 (6), 1272–1310.
- Belward, J., Turner, I., Oqielat, M., 2008. Numerical Investigation of Linear Least Square Methods for Derivatives Estimation. CTAC 08 Computational Techniques and applications conference, Australia, July 2008.
- Borga, M., Vizzaccaro, A., 1997. On the interpolation of hydrologic variables: formal equivalence of multiquadric surface fitting and kriging. *J. Hydrol.* 195, 160–171.

- Carlson, R.E., Foley, T.A., 1991. The parameter R2 in multiquadric interpolation. *Comput. Math. Appl.* 21, 29–42.
- Carr, J.C., Fright, W.R., Beatson, R.K., 1997. Surface interpolation with radial basis functions for medical imaging. *IEEE Trans. Med. Imaging* 16 (1), 96–107.
- Carr, J.C., Beatson, R.K., Cherrie, J.B., Mitchell, T.J., Fright, W.R., McCallum, B.C., Evans, T.J., 2001. Reconstruction and Representation of 3D Objects with Radial Basis Functions. *ACM SIGGRAPH*, 12–17 August 2001, Los Angeles, CA, pp. 67–76.
- Carr, J.C., Beatson, R.K., McCallum, B.C., Fright, W.R., McLennan, T.J., Mitchell, T.J., 2003. Smooth surface reconstruction from noisy range data. In: *ACM Graphite2003*, 11–14 February 2003, Melbourne, Australia, pp. 119–126.
- Cherrie, J., 2000. *Fast Evaluation of Radial Basis Functions: Theory and application* (Ph.D. thesis). University of Canterbury, New Zealand.
- Clough, R.W., Tocher, J.L., 1965. Finite element stiffness matrices for analysis of plate bending. In: *Proceedings of the Conference on Matrix Methods in Structural Mechanics*. Wright-Patterson A.F.B., Ohio, pp. 515–545.
- Davydov, O., Zeilfelder, F., 2004. Scattered data fitting by direct extension of local polynomials to bivariate splines. *Adv. Comput. Math.* 21 (3–4), 223–271.
- Dorr, G., Kempthorne, D., Mayo, L.C., Forster, W.A., Zabkiewicz, J.A., McCue, S.W., Belward, J.A., Turner, I.W., Hanan, J., 2014. Towards a model of spray-canopy interactions: interception, shatter, bounce and retention of Droplets on horizontal leaves. *Ecol. Model.* 290, 94–101. <http://dx.doi.org/10.1016/j.ecolmodel.2013.11.002>.
- Espana, M., Baret, F., Aries, F., Andrieu, B., Chelle, M., 1999. Radiative transfer sensitivity to the accuracy of canopy structure description. the case of a maize canopy. *Agronomie* 19, 241–254.
- Foley, T., 1987. Interpolation and approximation of 3-D and 4-D scattered data. *Comput. Math. Appl.* 13, 711–740.
- Franke, R., 1982. Scattered data interpolation: tests of some methods. *Math. Comput.* 38 (157).
- Hardy, R., 1990. Theory and applications of the multiquadric-biharmonic method. *Comput. Math. Appl.* 19, 163–208.
- Junkins, J., Miller, G.W., Jancaitis, J.R., 1971. A weighting function approach to modeling of irregular surfaces. *J. Geophys. Res.* 78, 1794–1803.
- Kempthorne, D., Turner, I.W., Belward, J.A., McCue, S.W., Barry, M., Young, J., Dorr, G. J., Hanan, J., Zabkiewicz, J.A., 2015. Surface reconstruction of wheat leaf morphology from three-dimensional scanned data. *Funct. Plant Biol.* 42, 444–451 (10.1071/FP14058).
- Kempthorne, D., Turner, I.W., Belward, J.A., 2015. A comparison of techniques for the reconstruction of leaf surfaces from scanned data. *SIAM J. Sci.*
- Lancaster, P., Salkauskas, K., 1986. *Curve and Surface Fitting, An Introduction*. Academic Press, San Diego.
- Loch, B., 2004. *Surface Fitting for the Modelling of Plant Leaves* (Ph.D. thesis). University of Queensland.
- Micchelli, C., 1984. Interpolation of scattered data: distance matrices and conditionally positive definite functions. *Constr. Approx.* 2, 11–22.
- Moroney, T., 2006. *An Investigation of a Finite Volume Method Incorporating Radial Basis Functions for Simulating Nonlinear Transport* (Ph.D. Thesis), Australia, <<http://www.sci.qut.edu.au/about/staff/mathsci/computational/moroneyt.jsp>>.
- Niceno, B., 2003. Easymesh. <<http://www-dinma.univ.trieste.it/nirftc/research/easymesh>>.
- Oqielat, M., Belward, J.A., Turner, I.W., Loch, B.I., 2007. A hybrid Clough-Tocher radial basis function method for modelling leaf surfaces. In: *MODSIM 2007 International Congress on Modelling and Simulation*. Modelling and Simulation Society of Australia and New Zealand, pp. 400–406.
- Oqielat, M., Belward, J.A., Turner, I.W., 2009. A hybrid clough-tocher method for surface fitting with application to leaf data. *Appl. Math. Model.* 33, 2582–2595.
- Oqielat, M., Turner I.W., M.N., Belward, J.A., McCue, S.W., 2011. Modelling water droplet movements on a leaf surface. *Math. Comput. Simul.* 81, 1553–1571. <http://dx.doi.org/10.1016/j.matcom.2010.09.003>.
- Powell, M., 1990. *The Theory of Radial Basis Function Approximation in 1990*. Advances in Numerical Analysis, Wavelets, Subdivision Algorithms and Radial Functions. W. Light.
- Prusinkiewicz, P., 1998. Modelling of spatial structure and development of plants: a review. *Sci. Hortic.* 74, 113–149.
- Rippa, S., 1999. An algorithm for selecting a good value for the parameter c in radial basis function interpolation. *Adv. Comput. Math.* 11, 193–210.
- Room, P., Hanan, J., Prusinkiewicz, P., 1996. Virtual plants: new perspectives for ecologists, pathologists and agricultural scientist. *Trends Plant Sci.* 1 (1), 33–38.
- Sedgewick, R., 1988. *Algorithms*. Addison-Wesley, Reading, Mass.
- Sinoquet, H., Thanisawanyangkura, S., Mabrouk, H., Kasemsap, P., 1998. Characterization of the light environment in canopies using 3D digitising and image processing. *Ann. Bot.* 82, 203–212.
- Tony, F., Chan, Christian, H.P., 1990. Computing truncated singular value decomposition least squares solutions by rank revealing qr-factorizations. *SIAM J. Sci. Stat. Comput.* 11 (3), 519–530.
- Turner, I., Belward, J., Oqielat, M., 2008. Error bounds for least square gradients estimates. *SIAM J. Sci. Comput.*